The Journal of Immunology

DAP12-Based Activating Chimeric Antigen Receptor for NK Cell Tumor Immunotherapy

Katrin Töpfer, Marc Cartellieri, Susanne Michen, Ralf Wiedemuth, Nadja Müller, Dirk Lindemann, Michael Bachmann, Monika Füssel, Gabriele Schackert and Achim Temme

J Immunol 2015; 194:3201-3212; Prepublished online 4 March 2015;
doi: 10.4049/jimmunol.1400330
http://www.jimmunol.org/content/194/7/3201

The Journal of Immunology is published twice each month by
The American Association of Immunologists, Inc.,
1451 Rockville Pike, Suite 650, Rockville, MD 20852

Print ISSN: 0022-1767 Online ISSN: 1550-6606.

DAP12-Based Activating Chimeric Antigen Receptor for NK Cell Tumor Immunotherapy

Katrin Töpfer,* Marc Cartellieri,† Susanne Michen,* Ralf Wiedemuth,* Nadja Müller,* Dirk Lindemann,‡ Michael Bachmann,† Monika Füssel,§ Gabriele Schackert,* and Achim Temme*,¶

NK cells are emerging as new effectors for immunotherapy of cancer. In particular, the genetic engraftment of chimeric Ag receptors (CARs) in NK cells is a promising strategy to redirect NK cells to otherwise NK cell–resistant tumor cells. On the basis of DNAX-activation protein 12 (DAP12), a signaling adaptor molecule involved in signal transduction of activating NK cell receptors, we generated a new type of CAR targeting the prostate stem cell Ag (PSCA). We demonstrate in this article that this CAR, designated anti–PSCA-DAP12, consisting of DAP12 fused to the anti-PSCA single-chain Ab fragment scFv(AM1) confers improved cytotoxicity to the NK cell line YTS against PSCA-positive tumor cells when compared with a CAR containing the CD3ζ signaling chain. Further analyses revealed phosphorylation of the DAP12-associated ZAP-70 kinase and IFN-γ release of CAR-engineered cells after contact with PSCA-positive target cells. YTS cells modified with DAP12 alone or with a CAR bearing a phosphorylation-defective ITAM were not activated. Notably, infused YTS cells armed with anti–PSCA-DAP12 caused delayed tumor xenograft growth and resulted in complete tumor eradication in a significant fraction of treated mice. The feasibility of the DAP12-based CAR was further tested in human primary NK cells and confers specific cytotoxicity against KIR/HLA-matched PSCA-positive tumor cells, which was further enhanced by KIR-HLA mismatches. We conclude that NK cells engineered with DAP12-based CARs are a promising tool for adoptive tumor immunotherapy. ***The Journal of Immunology*****, 2015, 194: 3201–3212.**

One promising strategy to provide defined tumor reactivity to immune effector cells (i.e., T cells, NK cells) is the genetic modification with tumor-specific chimeric Ag receptors (CARs). These CARs recognize tumor-associated Ags on the surface of tumor cells and transmit activating signals into the immune effector cells. Recently, treatment of B cell leukemia patients with CAR-engineered T cells resulted in a successful clearance of leukemic cells, providing clinical evidence for the capability of this immunotherapeutic approach (1–3). Although a large number of studies demonstrated the in vitro and in vivo efficiency of CAR-modified T cells, fewer approaches examined the anti-tumor potential of CAR-engineered NK cells. Unlike T cells, NK cells are characterized by simultaneous expression of various inhibitory and activating receptors (4, 5). Interactions of inhibitory receptors with HLA class I molecules on autologous normal cells induce dominant negative signals that override activating signals and therefore prevent cytotoxic activity (6). Among inhibitory receptors, Ig-like transcript 2 recognizes all HLA class I molecules on somatic cells by engaging the conserved β_2-microglobulin and α3 domain of HLA class I molecules (7). As another form of self-presentation, the inhibitory heterodimer CD94/NKG2A binds to the nonclassical HLA-E, which presents a peptide derived from the signal peptide (SP) of HLA class I molecules (8, 9). Finally, polymorphic killer Ig-like receptors (KIRs)—for instance, the inhibitory KIR2DL2/3 and KIR2DL1—recognize C1 and C2 ligands from the HLA-C locus, respectively, in an allelic fashion (10, 11). Yet, two other inhibitory KIRs and their ligands, KIR3DL1, which recognizes the Bw4 motif of HLA-B alleles and of some HLA-molecules and KIR3DL2, which binds to certain HLA-A3 and HLA-A11 molecules, have been described (12–15). KIRs are clonally expressed on NK cells, which in combination with differentially expressed inhibitory and activating receptors of the C-type lectin family and members of the natural cytotoxicity receptor family, extends the NK cell subset repertoire (5). The absence of HLA class I expression (missing self), which is a well-known characteristic for virally infected and virally transformed tumor cells, dramatically decreases the threshold for NK cell activation (16). NK cells sensing missing self and simultaneously receiving appropriate activating signals, clonally expand (17, 18), release cytokines such as IFN-γ (5), and kill target cells via the perforin-granzyme pathway (19) or by action of death-receptor ligands (19, 20). Although under normal conditions NK cells are unresponsive to self, CAR-engineered NK cells are capable of killing tumor cells expressing the appropriate cell surface Ag.

Of interest, most CAR constructs used so far for the modification of NK cells contained the intracellular proportion of the CD3ζ signaling chain and conferred specific cytotoxicity to target cells with surface expression of the cognate tumor-associated Ag (21–23). In NK cells, the CD3ζ homodimer transmits signals after

*Section of Experimental Neurosurgery and Tumor Immunology, Department of Neurosurgery, University Hospital Carl Gustav Carus, TU Dresden, 01307 Dresden, Germany; †Institute of Radiopharmaceutical Cancer Research, Helmholtz-Zentrum Dresden-Rossendorf, 01328 Dresden, Germany; ‡Institute of Virology, Medical Faculty Carl Gustav Carus, TU Dresden, 01307 Dresden, Germany; §DKMS Life Science Lab, GmbH, 01307 Dresden, Germany; and ¶German Cancer Consortium (DKTK), 01307 Dresden, Germany

Received for publication February 6, 2014. Accepted for publication January 22, 2015.

This work was supported by Deutsche Krebshilfe e.V. Grant Az.: 109377 (to A.T.).

Address correspondence and reprint requests to Prof. Dr. Achim Temme, Department of Neurosurgery, Section of Experimental Neurosurgery and Tumor Immunology, University Hospital Carl Gustav Carus, TU Dresden, Fetscherstrasse 74, 01307 Dresden, Germany. E-mail address: Achim.Temme@uniklinikum-dresden.de

The online version of this article contains supplemental material.

Abbreviations used in this article: CAR, chimeric Ag receptor; DAP12, DNAX-activation protein 12; GvH, graft-versus-host; IRES, internal ribosomal entry site; KIR, killer Ig-like receptor; PSCA, prostate stem cell Ag; SFFV, spleen focus–forming virus; SP, signal peptide; TREM, triggering receptor expressed on myeloid cell members; wt, wild-type.

www.jimmunol.org/cgi/doi/10.4049/jimmunol.1400330

binding of the low-affinity FcγRIII (CD16) to IgG-opsonized targets, thereby inducing Ab-dependent cellular cytotoxicity. Likewise, the activation of CD3ζ-based CARs led to an Ab-dependent cellular cytotoxicity–like activity of CAR-modified NK cells when engaging target cells (21, 23). To establish a CAR that is not involved in CD3ζ-signaling and that provides an alternative route to activate NK cells, we focused on DNAX-activation protein 12 (DAP12) as a signaling domain. Because DAP 12 contains only one ITAM, it was also of special interest, whether a DAP12 domain can provide sufficient signaling to induce NK cell activation, compared with a CAR containing the CD3ζ-chain with three ITAMs.

In the immune system, DAP12 is found in cells of the myeloid lineage, such as macrophages and granulocytes, where it associates, for instance, with the triggering receptor expressed on myeloid cell members (TREM) and MDL1 (myeloid DAP12-associating lectin 1/*CLEC5A*), both involved in inflammatory responses against pathogens like viruses and bacteria (for review, see Ref. 24) (25). In the lymphoid lineage, DAP12 is expressed in NK cells and associates with activating receptors such as the C-type lectin receptor NKG2C (26), the natural cytotoxicity receptor NKp44 (27), and the short-tailed KIR3DS1 (28) and KIR2DS1/2/5, respectively (29–31). In particular, NGK2C is the dominant activating NK cell receptor for controlling CMV infection in both humans and mice (32–34). Therefore, we hypothesized that in NK cells a DAP12-containing CAR should generate sufficient activating signals upon cross-linking with its Ag.

In this study, we generated a DAP12-based CAR, designated anti–prostate stem cell Ag (PSCA)–DAP12, for redirecting NK cells toward PSCA-positive tumor cells. As a PSCA-binding moiety, we used our recently described single-chain fragment variable scFv(AM1) derived from the hybridoma 7F5 (35). PSCA represents a prostate- and prostate cancer–associated GPI-anchored cell surface Ag (36–39) that is predominantly expressed in normal prostate-specific tissue and overexpressed in prostate cancer specimens, including high-grade prostatic intraepithelial neoplasia and androgen-dependent/-independent tumors (39). Recently, PSCA was also found to be expressed in prostate cancer metastases (40) and prostate-unrelated carcinomas such as renal clear cell carcinoma (41), pancreatic adenocarcinoma (42), and glioblastoma (43). PSCA has been successfully used as target molecule for various immunotherapeutic approaches (37, 38, 44–46). In this article we show that the DAP12-based CAR led to ZAP-70 phosphorylation upon cross-linking with its Ag and therefore efficiently reprogrammed the cytotoxicity of YTS-NK cells toward otherwise resistant PSCA-positive tumor cells in vitro and in vivo. Interestingly, YTS-NK cells modified with the DAP12-based CAR showed a gradually improved specific cytotoxicity when compared with NK cells expressing a CD3ζ-based CAR. Furthermore, we demonstrate also that human primary NK cells can efficiently be modified with a anti–PSCA-DAP12 CAR and therefore acquire specific cytotoxicity against KIR/HLA-matched PSCA-positive tumor cell lines in vitro. In conclusion, our results suggest that DAP12-based CARs are suitable for the development of a NK cell–based immunotherapy for solid tumors.

Materials and Methods

Cells and generation of PSCA$^+$ target cell lines

The human embryonic kidney cell line 293T, the prostate cancer cell line PC3, and the glioma cell line H4 were engineered to express PSCA by lentiviral gene transfer. The resulting cell lines were designated 293T^{PSCA}, PC3^{PSCA}, and H4^{PSCA}. The 293T cells were maintained in DMEM (PAA, Cölbe, Germany) supplemented with 10% v/v heat-inactivated FBS (PAA), 10 mM HEPES (PAA), 100 U ml^{-1} penicillin, and 0.1 mg ml^{-1} streptomycin (PAA). The PC3 and the permanent IL-2–independent NK cell line YTS (47) cells were maintained in RPMI 1640 (PAA) with 10% v/v heat-inactivated FBS (PAA), 2 mM L-glutamine (Biochrom, Berlin, Germany), 10 mM HEPES (PAA), 100 U ml ml^{-1} penicillin, and 0.1 mg ml^{-1} streptomycin (PAA). H4 cells were cultured in BME Life Technologies (Life Technologies, Darmstadt, Germany) with 10% v/v heat-inactivated FBS (PAA), 2 mM L-glutamine (Biochrom), 10 mM HEPES (PAA), 100 U ml^{-1} penicillin, 0.1 mg ml^{-1} streptomycin (PAA), and 1× MEM NEAA (nonessential amino acids; PAA). The PSCA-positive bladder carcinoma cell lines RT4 and HT1376 were grown in DMEM (PAA) supplemented with 10% v/v heat-inactivated FBS (PAA), 10 mM HEPES (PAA), 100 U ml^{-1} penicillin, 0.1 mg ml^{-1} streptomycin (PAA), and 1× MEM NEAA (PAA). All cell lines were cultivated at 37°C and 5% CO_2 in a humidified incubator.

Generation of lentiviral CAR vectors

To generate DAP12- and CD3ζ-based CARs, a fragment consisting of the Igkappa SP and the anti-PSCA single-chain fragment variable scFv(AM1) (35) was amplified by PCR using specific primers, adding a C-terminal short peptide linker $(Gly2Ser1)_2$. The PCR fragment was ligated into the lentiviral self-inactivating vector p6NST50 (48), resulting in p6NST50-anti–PSCA. A spleen focus–forming virus (SFFV) U3 promoter allowed transgene expression in combination with expression of an EGFP-Zeo^R reporter gene via an internal ribosomal entry site (IRES). The coding region of CD3ζ without TM domain and the transmembrane and hinge domains of CD28 were derived from reverse-transcribed human T cell mRNAs. Both were amplified by PCR and fused using appropriate restriction sites to generate a CD28 hinge-TM-CD3ζ fragment. The coding region of DAP12 was derived from CMV-SPORT6-IRATp970H1012D (containing the full-length cDNA for DAP12, provided by the I.M.A.G. E. Consortium and the Deutsches Resourcenzentrum für Genomforschung, Berlin, Germany). With PCR, appropriate restriction sites and a myc-tag were added to the signaling adaptor proteins flanked by short (Gly2Ser1) linkers. These signaling adaptor proteins were ligated in frame with scFv (AM1) of p6NST50 to generate the lentiviral CAR vectors p6NST50-anti–PSCA-DAP12-IRES-EGFP-Zeo^R and p6NST50-anti–PSCA-CD3ζ-IRES-EGFP-Zeo^R. To generate controls devoid of the Ag-binding moiety and containing only the signal adaptor, the Igkappa SP was fused to myc-CD3ζ and myc-DAP12, respectively, and resulting fragments were cloned into p6NST50, creating the lentiviral vectors p6NST50-myc-DAP12-IRES-EGFP-Zeo^R and p6NST50-myc-CD3ζ-IRES-EGFP-Zeo^R. A DAP12 with a phosphorylation-deficient ITAM was generated by PCR of p6NST50-anti–PSCA-DAP12-IRES-EGFP-Zeo^R,using the primers DAP12mut-For 5′-TTTTTGCATGCGTTAACGAACAAAAACTCATCTCAGAAGAGG-3′ and DAP12mut-p6NST50-Rev 5′-GAGTCGCCTTCTCAGGAGCTCCA-GGGTCAGAGGTCGGATGTCTC TAGCGACCTCAACACACAGAGG-CCGTATACAAATGAGCGGCCGCTTTTT-3′ (Eurofins MWG Operon), resulting in the DAP12mut fragment. This fragment was used to construct p6NST50-anti–PSCA-mutDAP12-IRES-EGFP-Zeo^R. For transduction of primary NK cells, we used a p6NST1-derived (48) self-inactivating lentiviral pHATtrick vector (K. Töpfer, R. Wiedemuth, and A. Temme, manuscript in preparation) devoid of the WPRE (49) and containing an internal SSFV U3 promoter followed by a multiple cloning site and a T2A Thosea assigna virus element fused in frame to EGFP. The coding regions for anti–PSCA-DAP12 CAR and myc-DAP12 control were ligated in frame to the T2A-EGFP, creating lentiviral vectors pHATtrick-anti–PSCA-DAP12-T2A-EGFP and pHATtrick-myc-DAP12-T2A-EGFP, respectively. All vectors were confirmed by DNA sequencing.

Virus production and transduction of NK cells

Lentiviral particles for transduction of YTS cells and primary NK cells were produced by a transient three-vector packaging protocol (50). Briefly, 4 × 10^6 293T cells were transfected using polyethylenimine (Polysciences, Warrington, PA), 5 μg pCD/NL-BH (50), pczVSV-G (51), and lentiviral vector, respectively. After 20 h, 293T cells were incubated with 10 mM sodium butyrate (Sigma-Aldrich, Taufkirchen, Germany) for 6 h. At 24 h after the replacement of sodium butyrate by fresh medium, the lentiviral supernatant was removed from cells and passed through a 0.45-μm filter, mixed with 8 μg ml^{-1} Polybrene (Sigma-Aldrich) and used to transduce NK cells. To enhance the expression of transgenes, YTS cells were selected in 5 mg ml^{-1} Zeocin (Invitrogen, Karlsruhe, Germany) for 1 wk. The use of human NK cells was approved by the local ethical committee (#EK242102007) of the Medical Faculty Carl Gustav Carus, Technische Universität Dresden. Human PBMCs were isolated either from buffy coats supplied by the German Red Cross (Dresden, Germany) or from fresh blood of healthy donors, after obtaining oral and written consent, by Biocoll gradient centrifugation (Biochrom, Berlin, Germany). Using the

negative NK Cell Isolation Kit (Miltenyi Biotec, Bergisch Gladbach, Germany), we isolated NK cells from human PBMCs. Staining with anti-CD3 and anti-CD56 Abs routinely confirmed ≥90% purity of $CD56^+$ and depletion of $CD3^+$ cells. The NK cells were cultured overnight in complete CellGro medium (CellGenix) supplemented with 500 U/ml IL-2 Proleukin S (Novartis) and expanded using the NK Cell Expansion Kit (Miltenyi Biotec). Transduction was repeated on 2 subsequent days using either a spinoculation protocol or a modified protocol according to Sutlu et al. (52). Briefly, 1×10^5 NK cells per well were seeded in a 48-well plate (Corning) and mixed with 1.5 ml virus supernatant, 500 U/ml Proleukin S, 20 ng/ml human IL-21 (Miltenyi Biotec), and 8 μg/ml Polybrene (Sigma-Aldrich). The plates were centrifuged at $805 \times g$ for 1 h at 20°C and further incubated at 37°C, 5% CO_2, for 5 h. After the third transduction, cells were maintained in CellGro GMP SCGM Medium supplemented with 10% FBS (Life Technologies), 500 U/ml Proleukin S, and 20 ng/ml human IL-21.

HLA typing

HLA alleles of donors and tumor cell lines were determined using high-resolution SSOP (Live Technologies Europe, Thermo Fisher Scientific, Heidelberg, Germany) and SPP (Olerup, Vienna, Austria) typing for HLA-A, -B, and -C. HLA-B and HLA-C mismatch predicting for a KIR-mismatch in the graft-versus-host (GvH) direction was calculated according to the published "missing ligand" model (11) and using KIR-ligand calculator software (www.ebi.ac.uk/ipd/kir/ligand.html).

Flow cytometry analyses of tumor cells and NK cells

The 7F5 mAb (35) and secondary Cy3-labeled anti-mouse Ab (1:50; Jackson ImmunoResearch, Suffolk, U.K.) were used to detect PSCA. Tumor cells incubated with secondary Ab alone served as control. For analyses of the cell surface expression of the CAR and controls, 3×10^5 modified YTS cells or NK cells, respectively, were centrifuged and stained with a biotin-labeled c-myc-tag–specific Ab (1:25; Miltenyi Biotec) and a secondary anti-biotin–PE or biotin–APC Ab, respectively (1:25; Miltenyi Biotec). As control, an IgG isotype was included. To determine the cell surface expression of CAR and control constructs, viable cells were gated and stained cells were measured by FACS and analyzed by FlowJo software version 7.6.5 (TreeStar, Ashland, OR).

Western blot analysis

Transduced YTS cells were lysed in lysis buffer (10 mM Tris-HCL, pH 8.0; 140 mM NaCl; 1% Triton X-100). Cell lysates were cleared by centrifugation, separated by SDS-PAGE under reducing conditions, and transferred on a Westran polyvinylidene difluoride membrane (Whatman, Dassel, Germany). The protein-loaded and blocked membrane was incubated with an anti–c-myc mAb (1:5000; Invitrogen) followed by a HRP-labeled rabbit anti-mouse secondary Ab (1:1000; Dako, Glostrup, Denmark). To investigate the signal transduction after cross-linking CAR with PSCA Ag, 4×10^6 YTS cells, $YTS^{myc\text{-}DAP12}$ cells, or $YTS^{anti\text{–}PSCA\text{-}DAP12}$ cells were incubated together with 3×10^5 $293T^{PSCA}$ cells or 293T wild-type (wt) cells. The incubation was performed in a 12-well plate in a final volume of 1 ml serum-free RPMI 1640. After 2 h, cells were centrifuged and lysed in lysis buffer supplemented with Phosphatase Inhibitor Cocktail 2 (1:100; Sigma-Aldrich). Lysates were separated and transferred onto blot membranes. Phosphorylated ZAP-70 was detected with a phospho-ZAP-70 (Tyr^{319}) Ab (1:1000; Cell Signaling, Danvers, MA) followed by an HRP-labeled goat anti-rabbit secondary Ab (1:2000; Dako). Equal loading of samples was determined by stripping and reprobing the membrane for total ZAP-70 (1:2000; Cell Signaling) as well as total α-tubulin (1:5000; Sigma-Aldrich). Membranes were visualized and documented using the Luminata Classico Western HRP substrate (Millipore) and the LAS 3000 imager (FujiFilm Europe). The specific phosphorylation of ZAP-70 upon binding of the CAR to its Ag was confirmed in three independent experiments.

Cytokine release assay

The release of IFN-γ after engagement of CAR-modified NK cells with PSCA-positive tumor cells was tested in a sandwich ELISA (OptEIA Human IFN-γ ELISA Kit II; BD Biosciences). In this procedure, 1×10^5 NK cells transduced with myc-DAP12 control and anti–PSCA-DAP12 CAR, respectively, were serum starved for 48 h and immediately confronted with 1×10^4 PSCA-positive tumor cells and PSCA-negative isogenic control cells, respectively, in a round-bottom 96-well plate in a final volume of 200 μl RPMI 1640 (without FBS). After 6 h and optionally 18 h, cells were spun down and supernatants were analyzed in duplicates according to the manufacturer's protocol. Data depicted in Fig. 3 represent the target-induced IFN-γ release mean values ± SEM in triplicates from at least two independent experiments.

Chromium release assay

The Ag-specific cytotoxicity of CAR-engineered NK cells toward PSCA-positive tumor cells was tested by chromium release assays. Briefly, 2×10^6 target cells were labeled with 50 μCi sodium chromate 51(PerkinElmer, Ueberlingen, Germany) and incubated at 37°C and 5% CO_2. After 1 h, cells were washed several times with PBS and seeded as triplicates in a round-bottom 96-well plate (5×10^3 cells per well). CAR-modified YTS cells and NK cells, as well as controls, were added to labeled target cells at various target to effector ratios. After 18 h, 25 μl cell supernatant was mixed with 150 μl of scintillation solution OptiPhase SuperMix (Wallac Scintillation Products, Turku, Finland) in a 96-well plate by shaking for 3–5 min at room temperature. The chromium release was measured using a Wallac 1450 Microbeta Trilux Liquid Scintillation and Luminescence Counter (PerkinElmer). Maximal and minimal releases were measured by treating target cells with 5% Triton X-100 (Serva, Heidelberg, Germany) and medium alone, respectively. Incubations of YTS cells and primary human NK cells with isogenic PSCA-negative cells were included for comparison. Percentage of specific lysis was calculated using the standard formula: 100 × (cpm release target cells − cpm minimum release) / (cpm maximum release − cpm minimum release). The experiments were performed three to four times using YTS cells and at least two times using primary NK cells from three donors, each with similar results.

Experimental immunotherapy of xenografted mice

$NMRI\text{-}Foxn1^{nu}/Foxn1^{nu}$ mice were obtained from the animal facility of the University of Dresden. Mice were held under standardized pathogen-free conditions with ad libitum access to food and water. Experiments were approved by the Landesdirektion Dresden under the auspices of the German Animal Protection Law. To establish tumors, 100 μl PBS containing 4×10^6 293T-PSCA cells were s.c. injected into the left flank of female $NMRI^{nu/nu}$ mice (10 mice per group). At day 4 the tumor reached an average size of ~10 mm^2, and i.v. injections with 5×10^6 nonmodified YTS cells, $YTS^{myc\text{-}DAP12}$ cells, and $YTS^{anti\text{–}PSCA\text{-}DAP12}$ cells were started. YTS cells were injected via the tail vein every 48 h or 72 h over a period of 8 wk. As a control for in vivo tumor cell growth, one group was not treated. The experiment was repeated three times with, in total, 25 or 26 mice per group, with similar results. Tumors were measured in two dimensions one or two times per week, using a digital caliper. Once the tumor exceeded 18 mm in any of the three perpendiculars or animals appeared to be in distress, mice were euthanized. The tumor area was calculated according to the formula of ellipse area: $1/4 \times \pi \times (a \times b)$. For the analysis of PSCA expression in 293T-PSCA xenografts treated with CAR-modified YTS cells, we compared Ag expression levels of tumors in all treatment groups. Therefore, randomly selected mice having tumors exceeding 18 mm were sacrificed, and tumors were excised at days 22, 22, 22, and 24 for non-treated tumors; days 22, 22, 28, and 28 after start of YTS treatment; days 22, 22, 24, and 34 after the start of $YTS^{myc\text{-}DAP12}$ treatment; and days 31, 42, 45, and 50 after the start of $YTS^{anti\text{–}PSCA\text{-}DAP12}$ treatment. The $293T^{PSCA}$ cells of the excised tumors were prepared using a Brain Tumor Dissociation Kit (Miltenyi Biotec) according to the instructions of the provider and were plated on 10-cm cell culture dishes for 24 h. After extensive washing with PBS, the remaining adherent cells were trypsinized; simultaneously stained for HLA-A,-B, and -C (HLA-ABC, clone REA230; Miltenyi Biotec) and PSCA or corresponding isotype controls; and analyzed by flow cytometry. In a further experiment, $293T^{PSCA/dsRed}$ xenografts were grown to a size of ~20 mm^2. Subsequently, two mice per group were i.v. injected with 5×10^6 YTS-DAP12 cells or YTS-anti–PSCA-DAP12 cells every 24 h, for a total of three times. At 24 h after the last injection, the mice were sacrificed and tumors were removed and transferred into embedding molds containing tissue-freezing medium (Leica, Wetzlar, Germany) and then snap frozen in dry ice. For microscopic examination, 10-μm slices were prepared with a microtome (Jung CM1800; Leica) and counterstained with DAPI. Digital images of tumors were acquired with the fluorescence microscope Axioskop 2 mot plus (Carl Zeiss, Göttingen, Germany; original magnification, ×200) and the AxioVision software version 8.0 (Carl Zeiss). For quantification of infiltrating EGFP-marked YTS cells, 12 randomly selected fields were counted for nuclei and EGFP-positive cells, and the percentage of infiltrating YTS cells was calculated.

Statistical analyses

The results of IFN-γ and chromium release assays were expressed as mean with SEM and analyzed performing a one-way ANOVA ($p < 0.05$) combined with a post hoc Tukey multiple comparison test ($p < 0.05$). A Student t test was used for comparison of tumor-infiltrating YTS cells. A log-rank test was used for analyses of the survival data. All statistical analyses were performed with Prism software version 6.0 (GraphPad Software, La Jolla, CA).

Results

Generation of YTS cells expressing the CAR anti–PSCA-DAP12

The design of the anti–PSCA-DAP12 chimeric NK cell Ag receptor and lentiviral vector regions is depicted in Fig. 1A. The DAP12-based CAR was generated by fusion of the recently described PSCA-specific single-chain fragment variable scFv(AM1) (35) to the extracellular domain of human DAP12. An internal SFFV U3 promoter allowed transgene expression in combination with expression of an EGFP-Zeo^R reporter gene via an internal IRES. Furthermore, we included an extracellular c-myc-tag for detection of CAR surface expression (Fig. 1A). To investigate a nonspecific activation of NK cells owing to an ectopic expression of the signaling adaptor protein DAP12, a control consisting of Igkappa SP fused to c-myc and DAP12 was included and referred to as myc-DAP12. As further control, we constructed a CAR containing a phosphorylation-defective ITAM (anti–PSCA-DAP12mut).

The NK cell line YTS, which is devoid of KIR expression (47, 53), was transduced with anti–PSCA-DAP12 CAR, anti–PSCA-DAP12mut control, and myc-DAP12 control, respectively. After antibiotic selection, the modified YTS cells expressed the CAR or control constructs, as shown by Western blot analyses (Fig. 1B). Protein bands consistent with the estimated molecular mass of ~46 kDa for anti–PSCA-DAP12 CAR and the signaling-deficient anti–PSCA-DAP12mut control, as well as 18 kDa for myc-DAP12 control, were detected using an anti–c-myc Ab (Fig. 1B). Furthermore, a strong surface expression of the CAR and of the control constructs, respectively, was detected in nearly all EGFP-marked YTS cells (Fig. 1C), which remained stable in a continuous culturing period of ≥5 mo (data not shown).

Specific killing of PSCA-positive tumor cell lines of different origin, using YTS cells engineered with anti–PSCA-DAP12 CAR

To investigate cytotoxicity of CAR-modified YTS cells, we used target cell lines with ectopic expression of PSCA but also chose HT1376 and RT4 cells with endogenous PSCA expression for our experiments. Flow cytometry analyses demonstrated robust endogenous expression of PSCA on RT4 and HT1376 bladder carcinoma cells and a high expression on PC3^{PSCA}, H4^{PSCA}, and 293T ^{PSCA} cells

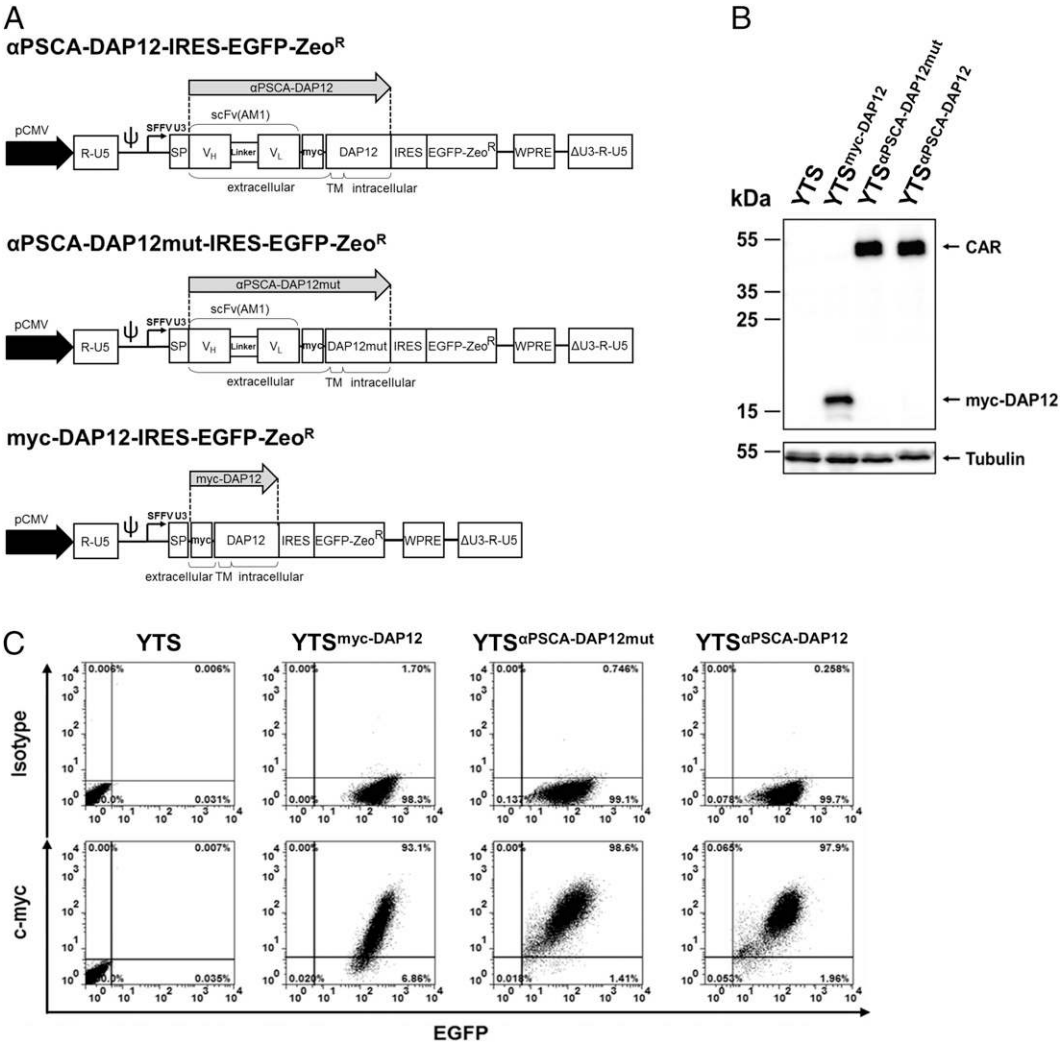

FIGURE 1. Engineering YTS cells with a DAP12-based CAR with specificity for PSCA. (**A**) Schematic representation of anti–PSCA-DAP12 CAR and anti–PSCA-DAP12mut coding sequences (gray arrow) in the lentiviral vector backbone. The anti–PSCA-DAP12mut harbors T91A and T102A mutations in its ITAM. The control construct myc-DAP12 lacks the PSCA-specific scFv(AM1). The internal SFFV U3 promoter of the provirus regulates the expression of the transgenes. Protein synthesis into the secretory pathway is provided by an Igkappa SP at the N terminus. Expression of the EGFP-ZEO^R is controlled by an IRES. (**B**) Immunoblot analysis of total protein lysates of transduced YTS cells demonstrating expression of the anti–PSCA-DAP12 CAR and the control constructs. The detection of CAR and controls was accomplished using a c-myc-tag–specific Ab and HRP-labeled anti-mouse secondary Ab. (**C**) The proper surface expression of the functional CAR and the controls as determined by flow cytometry analysis using anti–c-myc–biotin Ab and PE-labeled anti-biotin secondary Ab. Cells stained with IgG isotype Ab (*upper panels*) served as a control.

transduced with a vector encoding PSCA. Endogenous PSCA expression was not detectable in PC3, H4, and 293T wt cells (Fig. 2A). We performed chromium release assays to investigate the specific cytotoxicity of CAR-modified YTS$^{anti–PSCA-DAP12}$ against PSCA-positive tumor cells. As anticipated, PSCA-positive tumor cells were significantly lysed by YTS$^{anti–PSCA-DAP12}$ cells at different target to effector ratios when compared with control cells (***$p < 0.0001$; Fig. 2B). YTS$^{anti–PSCA-DAP12}$ cells showed an average tumor cell lysis ranging from 60% at a target to effector ratio of 1:2.5 to ~80% and higher at a target to effector ratio of 1:10. Of note, YTS$^{anti–PSCA-DAP12}$ cells killed the different PSCA-positive tumor cells at almost the same efficiency regardless of their origin and level of PSCA expression. As expected, incubation of YTS$^{anti–PSCA-DAP12}$ cells with PSCA-negative isogenic tumor cells did not lead to tumor cell lysis. Moreover, unmodified YTS cells, YTS$^{myc-DAP12}$ cells, and YTS$^{anti–PSCA-DAP12mut}$ cells lysed neither PSCA-positive nor PSCA-negative tumor cells. Taken together, these results clearly demonstrate that the anti–PSCA-DAP12 CAR confers specific cytotoxicity against PSCA-positive target cells from different tumor entities.

ZAP-70 phosphorylation and IFN-γ release in NK cells upon CAR cross-linking

The biochemical events accompanying stimulation of DAP12-associated receptors in NK cells are still not well characterized, but involve ZAP-70 and Syk protein tyrosine kinases, as shown for the activating human KIR2DS2 (31). We hypothesized that cross-linking of anti–PSCA-DAP12 CAR might also lead to an ITAM phosphorylation of the DAP12 portion within the CAR, leading to recruitment and phosphorylation of ZAP-70. Subsequently, activated ZAP-70 should trigger downstream signaling, which essentially contributes to NK cell activation and cytokine release (54). To test the capability of anti–PSCA-DAP12 CAR to induce ZAP-70 phosphorylation and cytokine release, we cocultured YTS$^{anti–PSCA-DAP12}$ cells with 293T^{PSCA} cells and 293T wt cells, respectively, and analyzed phosphorylation of ZAP-70. As additional controls, YTS and YTS$^{myc-DAP12}$ were included in the experiments. The Western blot analyses revealed equal steady state protein expression of total ZAP-70 protein in YTS$^{anti–PSCA-DAP12}$ cells as well as in control cells. Notably, we observed a robust phosphorylation of ZAP-70 only in YTS$^{anti–PSCA-DAP12}$ cells when incubated with 293T^{PSCA} cells, whereas phosphoZAP-70 was absent in cell lysates of YTS cells and YTS$^{myc-DAP12}$ cells (Fig. 3A). Moreover, when cocultured with PSCA-negative 293T wt cells, phosphoZAP-70 was not detectable in YTS$^{anti–PSCA-DAP12}$ cells or in YTS and YTS$^{myc-DAP12}$ cells, indicating that phosphorylation occurs only after cross-linking of the DAP12-based CAR with its Ag.

To assess whether phosphorylated ZAP-70 correlates to increased cytokine release (54), we analyzed secreted IFN-γ levels

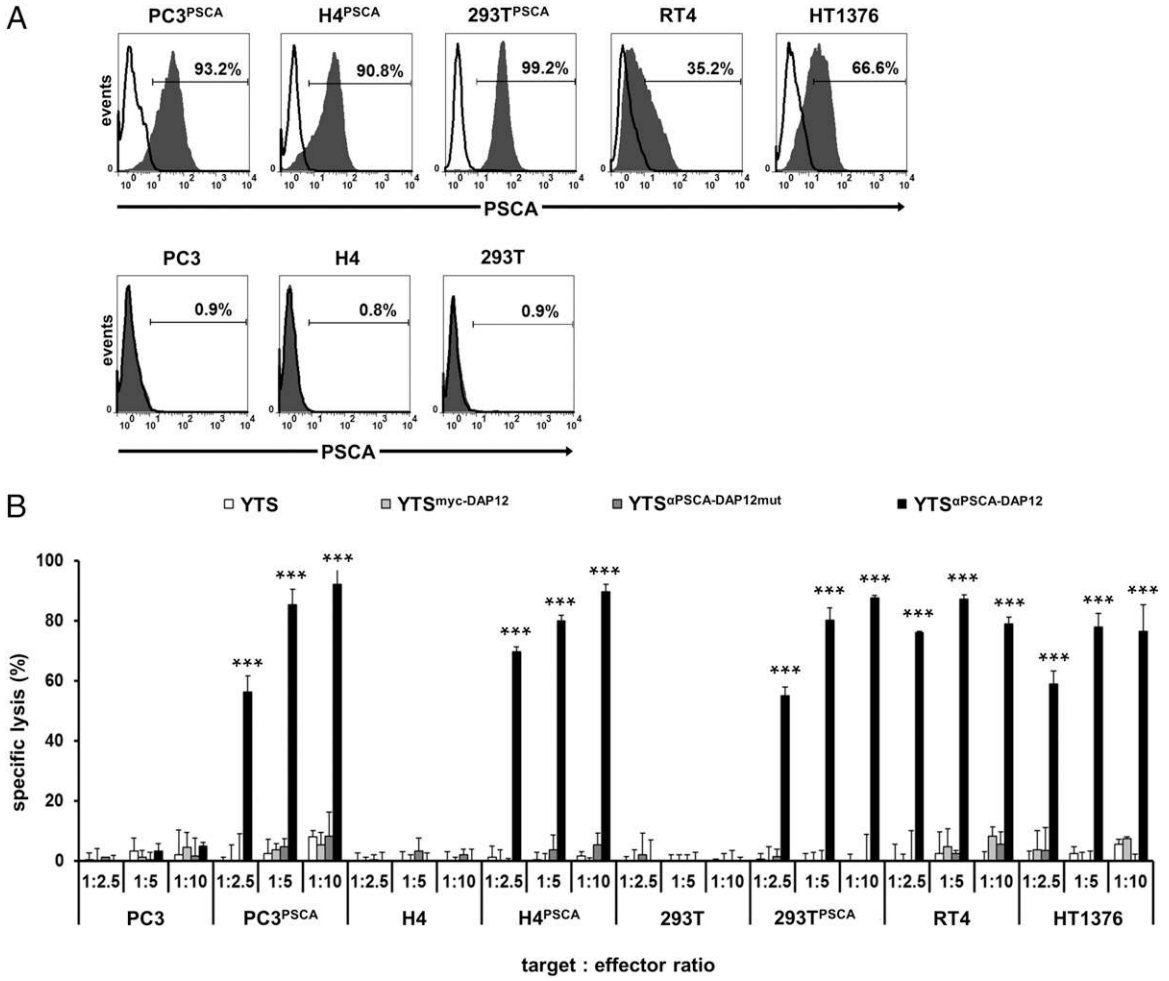

FIGURE 2. Specific cytotoxicity of anti–PSCA-DAP12 CAR–expressing YTS cells against PSCA$^+$ tumor cells. (**A**) PSCA-positive tumor cells (*upper panels*) and isogenic control cells (*lower panels*) were stained using a PSCA-specific 7F5 mAb and secondary Cy3-labeled anti-mouse Ab (gray histograms). An isotype control staining is included (open histograms) (**B**) Gene-engineered and parental YTS cells were cocultured with sodium chromate 51–loaded PSCA-expressing tumor cells and isogenic PSCA-negative control cells at different target to effector ratios for 18 h. The mean of specific tumor cell lysis and SD of triplets of one representative chrome release assay are shown. Note the strong tumor cell lysis mediated by YTS-anti–PSCA-DAP12 cells. ***$p < 0.0001$.

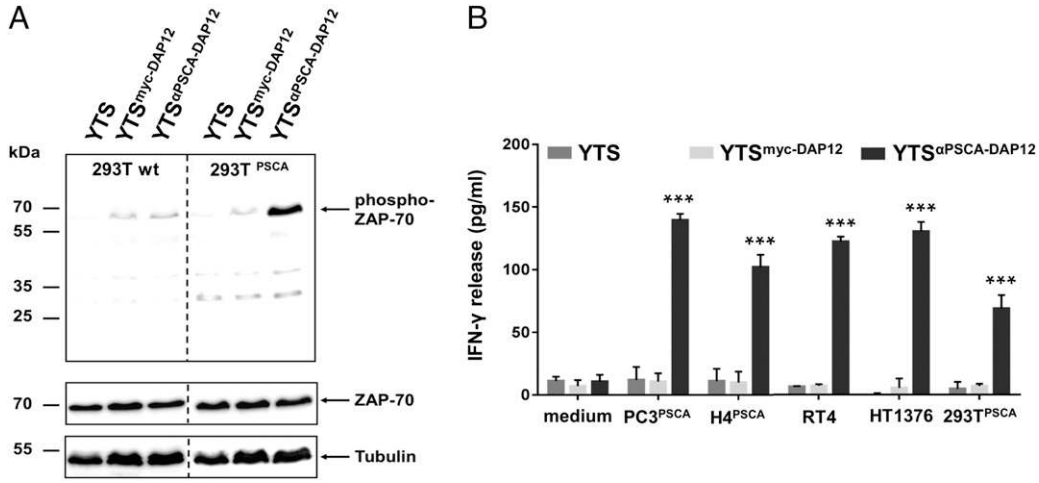

FIGURE 3. Cross-linking with PSCA-expressing tumor cells induced phosphorylation of ZAP-70 and increased IFN-γ release in CAR-engineered YTS cells. (**A**) Total protein lysates of YTS cells, YTS$^{myc\text{-}DAP12}$ cells, or YTS$^{anti\text{–}PSCA\text{-}DAP12}$ cells cocultured with either 293T cells or 293T^{PSCA} cells were subjected to Western blot analysis. Phosphorylated ZAP-70 was detected only in YTS$^{anti\text{–}PSCA\text{-}DAP12}$ cells after incubation with PSCA-positive target cells. Equal ZAP70 expression was confirmed after stripping of the protein-loaded membrane and reprobing with an anti–ZAP-70 Ab. Tubulin staining was included as an additional loading control. (**B**) YTS, YTS$^{myc\text{-}DAP12}$, and YTS$^{anti\text{–}PSCA\text{-}DAP12}$ cells were incubated with PSCA-positive tumor cell lines PC3^{PSCA}, H4^{PSCA}, 293T^{PSCA}, RT4, or HT1376. In addition, nontransduced YTS cells were included in the experiment. After 6 h of incubation, cell-free supernatant was harvested and the amount of released IFN-γ was measured by sandwich ELISA. Mean IFN-γ release and SD of triplets are shown. $***p < 0.0001$.

of YTS$^{anti\text{–}PSCA\text{-}DAP12}$ cells after a 6-h confrontation with PSCA-positive tumor cells. As control, we included YTS and YTS$^{myc\text{-}DAP12}$ cells. As anticipated, in the presence of PSCA-expressing tumor cells, the YTS cells engineered with anti–PSCA-DAP12 CAR showed a significant increase of IFN-γ release ($***p < 0.0001$; Fig. 3B). YTS$^{anti\text{–}PSCA\text{-}DAP12}$, which had been cultivated with PC3^{PSCA} cells, released the highest amount of IFN-γ (140 pg/ml). Lower concentrations of IFN-γ were found in the supernatant of YTS$^{anti\text{–}PSCA\text{-}DAP12}$ cells cocultured with H4^{PSCA} (102 pg/ml), RT4 cells (122 pg/ml), or HT1376 cells (130 pg/ ml). YTS$^{anti\text{–}PSCA\text{-}DAP12}$ cells confronted with 293T^{PSCA} cells released the lowest amount of IFN-γ (68 pg/ml). In contrast, YTS cells and YTS$^{myc\text{-}DAP12}$ control cells did not release IFN-γ when cocultured with the PSCA-positive target cells. In conclusion, these data indicate that cross-linking of the PSCA-specific CAR with its Ag causes ZAP-70 phosphorylation and downstream signaling events, resulting in IFN-γ release.

Comparison of DAP12-CAR and CD3ζ-CAR formats

Because it was of special interest whether a DAP12-based CAR signals as efficiently as the mostly used NK-CAR format containing the CD3ζ-chain, we sought to compare the DAP12-based CAR with a CD3ζ-based CAR. We therefore constructed anti–PSCA-CD3ζ (Fig. 4A) and generated YTS$^{anti\text{–}PSCA\text{-}CD3\zeta}$ cells. As control, we included mock-transduced YTS cells expressing only the signaling adaptor CD3ζ. The analyses of CAR expression revealed equal levels of anti–PSCA-CD3ζ and anti–PSCA-DAP12 molecules on the surface of the transduced YTS cell lines (Fig. 4B). To compare the different types of CARs, we performed IFN-γ release assays and chromium release assays and included 293T^{PSCA} target cells and, as control, 293T wt cells. Furthermore, we used YTS cells, YTS$^{myc\text{-}DAP12}$ cells, and YTS$^{myc\text{-}CD3\zeta}$ cells to exclude any nonspecific side effect arising from ectopically expressed ITAM-containing protein domains. Of interest, YTS$^{anti\text{–}PSCA\text{-}DAP12}$ and YTS$^{anti\text{–}PSCA\text{-}CD3\zeta}$ released similar amounts of IFN-γ cells when confronted with 293T^{PSCA} cells at a target to effector ratio of 10:1, which was recapitulated using other PSCA-positive target cell lines (Supplemental Fig. 1). In a chromium release assay, both the DAP12-based CAR and the CD3ζ-based CAR specifically lysed PSCA-positive target cells, whereas 293T wt cells were not affected (Fig. 4C). In contrast, YTS cells, YTS$^{myc\text{-}DAP12}$ cells, and YTS$^{myc\text{-}CD3\zeta}$ cells showed no cytotoxicity against PSCA-positive or PSCA-negative target cells, which again confirms that ectopically expressed DAP12 and CD3ζ signaling proteins do not induce nonspecific NK cell cytotoxicity. Notably, we constantly observed an increased specific cytotoxicity ($*p < 0.05$) of YTS$^{anti\text{–}PSCA\text{-}DAP12}$ when compared with YTS$^{anti\text{–}PSCA\text{-}CD3\zeta}$ at the lower target to effector ratios of 1:2.5 and 1:5. Therefore, it appears that a DAP12-based CAR is slightly superior when compared with a CAR containing the CD3ζ signaling domain.

Antitumor effects of YTS$^{anti\text{–}PSCA\text{-}DAP12}$ cells injected into tumor-bearing mice

The in vivo antitumor effect of PSCA-specific YTS cells on established solid tumors was analyzed in a mouse xenograft tumor model. For this procedure, 293T^{PSCA} cells were s.c. injected into the left flank of female NMRI-Foxn1^{nu}/Foxn1^{nu} mice. Once the tumor developed, YTS cells, YTS$^{myc\text{-}DAP12}$ cells, and YTS$^{anti\text{–}PSCA\text{-}DAP12}$ cells, respectively, were given via the tail vein every 48 h or 72 h over a period of 8 wk, and the behavior and weight of animals were monitored daily. We chose this regimen because our initial experiments revealed only a transient and moderate control of tumor growth after a single injection of CAR-modified YTS cells or after prolonging the intervals between YTS injections (data not shown). That the CAR-modified YTS cells as well as the YTS$^{myc\text{-}DAP12}$ control cells reached the tumor was confirmed using DsRed-marked 293T$^{PSCA/dsRed}$ xenografts for better visualization. The experiments revealed an inhomogeneous and moderate infiltration and no differences in the numbers of tumor-infiltrating YTS$^{anti\text{–}PSCA\text{-}DAP12}$ cells when compared with YTS$^{myc\text{-}DAP12}$ cells (Supplemental Fig. 2). Through applying the aforementioned continuous treatment protocol, 14 of 26 mice receiving YTS$^{anti\text{–}PSCA\text{-}DAP12}$ cells showed a complete or near complete tumor eradication at day 45 after transplantation of the tumors, whereas no such effect was observed in the control groups. Overall, YTS$^{anti\text{–}PSCA\text{-}DAP12}$-treated mice showed a significant decrease in tumor growth when compared with all control groups ($***p < 0.0001$; Fig. 5A). In addition, the treated mice

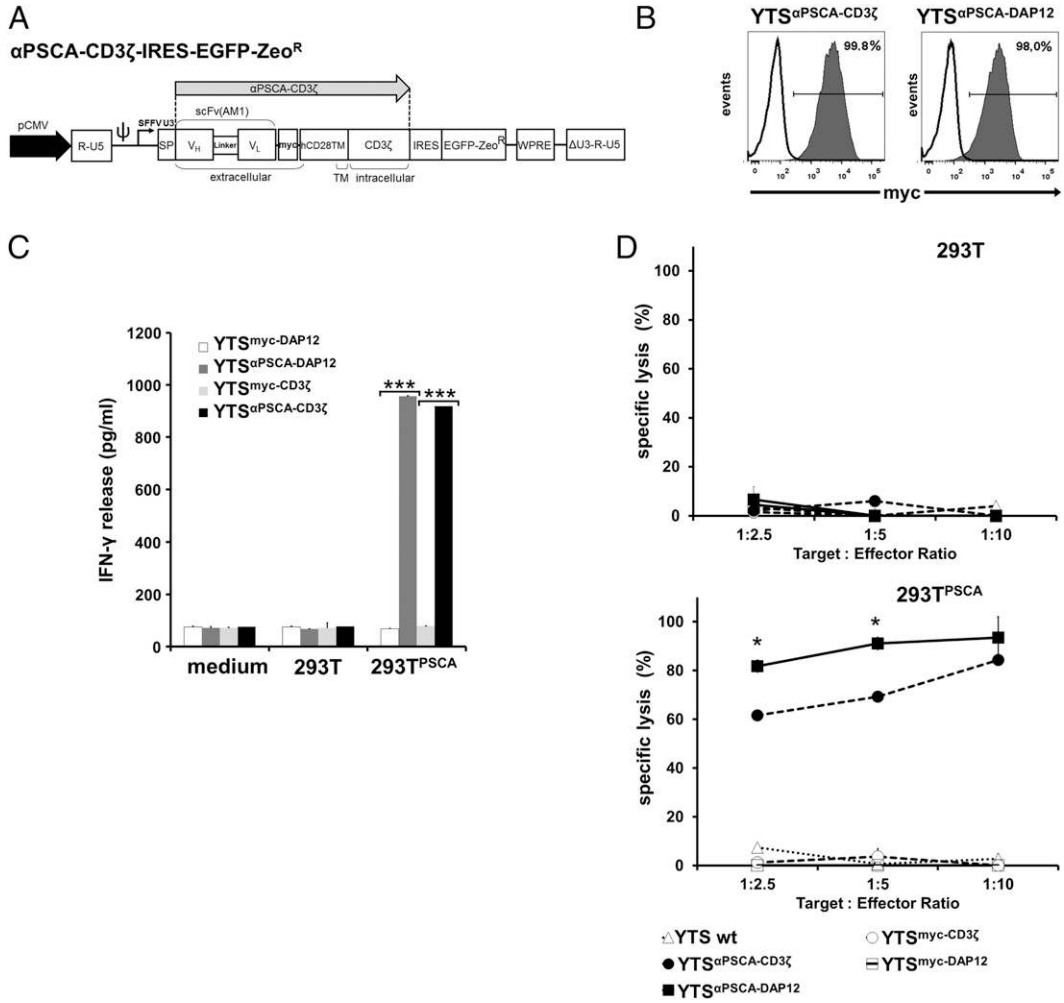

FIGURE 4. Comparison of DAP12- and CD3ζ-based anti-PSCA CARs. (**A**) Schematic representation of the anti–PSCA-CD3ζ CAR coding sequence (gray arrow) in the lentiviral vector backbone. To achieve an efficient surface expression of the CAR, the CD3ζ without transmembrane domain was fused to the hinge and TM domain of CD28 (hCD28TM). (**B**) Surface expression of transduced anti–PSCA-CD3ζ CAR in comparison with surface expression of the anti–PSCA-DAP12 CAR on transduced YTS cells (gray histogram). Isotype control staining is included (open histogram). Note the similar levels of surface expression of anti–PSCA-CD3ζ CAR and anti–PSCA-DAP12 CAR. (**C**) Transduced YTS$^{\text{anti–PSCA-DAP12}}$ and YTS$^{\text{anti–PSCA-CD3ζ}}$ and controls expressing only the DAP12 or CD3ζ signal adaptor were incubated with 293T$^{\text{PSCA}}$ and isogenic 293T control cells, respectively. After 18 h of incubation, cell-free supernatant was harvested and the amount of released IFN-γ was measured by sandwich ELISA. Depicted are the summarized results from two independent experiments with similar results. Note the increase in IFN-γ release of YTS$^{\text{anti–PSCA-DAP12}}$ (dark gray columns) and YTS$^{\text{anti–PSCA-CD3ζ}}$ cells (black columns) after cocultivation with PSCA-positive target cells. Mean IFN-γ release of four single measurements and SEM are shown. (**D**) Modified and YTS cells were cocultured with sodium chromate 51–loaded PSCA-expressing tumor cells and isogenic PSCA-negative control cells at different target to effector ratios for 18 h. The mean of specific tumor cell lysis and SEM of triplets of one representative chrome release assay are shown. $*p < 0.05$, $***p < 0.001$.

showed neither significant loss of weight nor altered behavior during the treatment. Of note, the injection of YTS$^{\text{anti–PSCA-DAP12}}$ cells caused a statistically significant increase in median survival time of 99 d in comparison with control groups (without YTS cells: 63 d; with YTS cells: 52 d; with YTS$^{\text{myc-DAP12}}$ cells: 86 d; $p < 0.001$). Moreover, 31% of mice with YTS$^{\text{anti–PSCA-DAP12}}$ treatment showed a complete and stable tumor regression and remained tumor free at the termination of the experiments at day 155 (Fig. 5B). To exclude a loss of PSCA-Ag as a potential immune evasion mechanism, randomly selected tumors were prepared to determine PSCA surface expression levels. Yet, tumor growth controls, tumors treated with control YTS, YTS$^{\text{myc-DAP12}}$, and YTS$^{\text{anti–PSCA-DAP12}}$, displayed no decrease in expression of PSCA (Supplemental Fig. 3). To investigate engraftment but also to exclude negative effects of YTS NK cells in mice (e.g., development of lymphoproliferative disease), the peripheral blood and bone marrow of three survivors that had received treatment with YTS$^{\text{anti–PSCA-DAP12}}$ cells were tested after termination of the experiment for circulating EGFP-positive YTS cells. In all cases, YTS cells were absent in the blood or bone marrow of analyzed mice (Supplemental Fig. 3). Likewise, additional analyses of spleens and livers revealed no residual EGFP-positive YTS cells (data not shown). Taken together, these data indicate, on the one hand, a profound antitumor effect of continuously administered YTS$^{\text{anti–PSCA-DAP12}}$ cells but, on the other hand, demonstrate the inability of YTS cells to stably engraft in NMRI-Foxn1$^{\text{nu}}$/Foxn1$^{\text{nu}}$ mice.

Primary NK cells genetically engineered to express a DAP12-CAR kill PSCA-expressing target cells

To assess whether a DAP12-based CAR is suitable for potential clinical use, we sought to generate primary NK cells from healthy donors with expression of anti–PSCA-DAP12 CAR and myc-DAP12 as a control. In many transduction efforts, using lentiviral vectors with the p6NST50 backbone, we obtained mean transduction efficiencies in NK cells <20%, and so we decided to use shorter and modified pHATtrick lentiviral vectors for transduction of primary NK cells (see *Materials and Methods*).

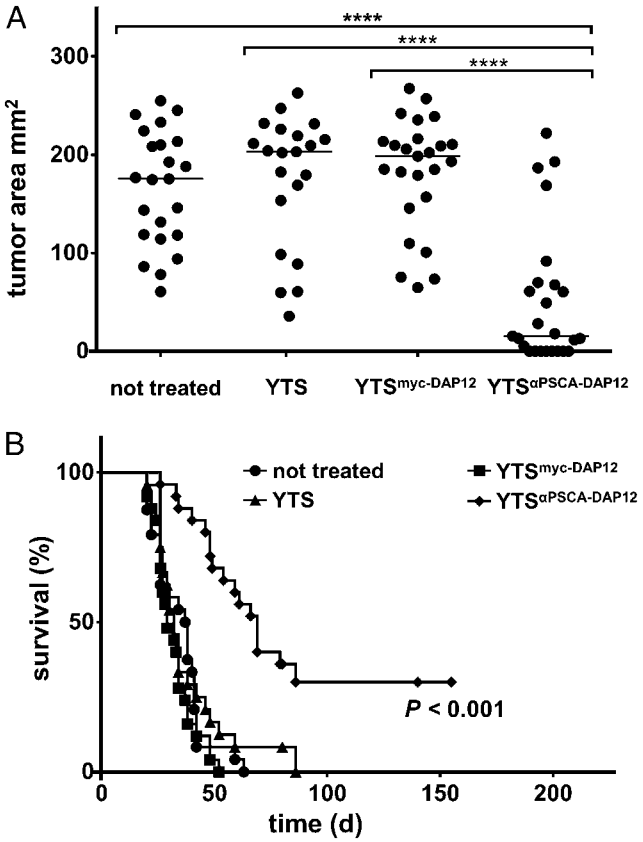

FIGURE 5. PSCA-redirected YTS cells led to regression of solid tumors in vivo. $293T^{PSCA}$ cells were s.c. injected into NMRI-$Foxn1^{nu}$/$Foxn1^{nu}$ mice. After tumor development, treatment of mice with i.v. tail vein injections of YTS cells, $YTS^{anti–PSCA-DAP12}$ cells, or $YTS^{myc-DAP12}$ cells was started. Nontreated mice were included as an additional control. (**A**) Mean tumor growth of living mice injected with $YTS^{anti–PSCA-DAP12}$ cells or control cells measured at day 45 after tumor transplantation. Note that a substantial fraction of $YTS^{anti–PSCA-DAP12}$-treated mice showed a complete or at least partial tumor regression. (**B**) Kaplan–Meier survival curve for overall survival of nontreated mice, mice injected with $YTS^{anti–PSCA-DAP12}$ or $YTS^{myc-DAP12}$ cells, and mice receiving control cells. Mice treated with $YTS^{anti–PSCA-DAP12}$ cells showed improved survival. Shown data summarize three independent experiments with similar results (n = 25 for YTS-treated mice; n = 26 for nontreated, $YTS^{myc-DAP12}$-treated, and $YTS^{anti–PSCA-DAP12}$-treated mice). $****p < 0.0001$.

pHATtrick contains a T2A-endoproteolytic cleavage site and EGFP after the CAR construct and myc-DAP12 control, respectively, as depicted in Fig. 6A. Flow cytometry analyses of EGFP expression levels revealed that transduced PBMC-derived NK cells from seven different donors expressed a mean of 50% (±10%) myc-DAP12 control or 48% (±16%) anti–PSCA-DAP12 CAR (Fig. 6B), with stable expression for ≥5 wk (data not shown). Yet, we constantly observed weakened mean fluorescence intensities when using myc-DAP12– and CAR-encoding vectors when compared with an empty vector control, which inversely correlates to the insert size of the lentiviral vectors. However, further analyses using an anti–c-myc-tag Ab revealed that ∼75% of $EGFP^+$ NK cells expressed the CAR and the myc-DAP12 control construct on the cell surface, respectively (Fig. 6C). To predict a possible allogeneic reactivity, the HLA genes of donors and target cells were genotyped (Supplemental Fig. 4B). We calculated that NK cells from our donors were fully compatible with PC3 cells. In addition, donor no. 2 was fully compatible with H4 glioma cells, whereas donors no. 1 and no. 2 had a Bw4 mismatch in the GvH direction. Of note, all donors showed a C1 or C2 mismatch in the GvH direction when matched to the HLA genotype of RT4 and HT1376 cells, sometimes with an additional Bw4 (ligand for KIR3DL1) or Bw6 mismatch (the latter represents a ligand with an yet unknown NK receptor). Subsequent FACS analyses showed strong surface expression levels of HLA-A, -B, -C molecules in all tumor cell lines (Supplemental Fig. 4A). In a next step, we analyzed the ability of transduced NK cells to recognize PSCA-positive target cells by performing an IFN-γ release assay. For this procedure, CAR and control-transduced NK cells from the donors were incubated with either the PSCA-negative wt cell lines PC3, H4 or the PSCA-positive isogenic counterparts $PC3^{PSCA}$ or $H4^{PSCA}$. In addition, we included the PSCA-positive cell lines RT4 and HT1376 cells having a C1 or C2 mismatch in the experiments. Fig. 6D summarizes the results of the experiments for each donor. The $NK^{anti–PSCA-DAP12}$ cells were stimulated by $H4^{PSCA}$, RT4, and HT1376 cells to secrete increased amounts of IFN-γ (3000–4300 pg/ml) (Fig. 6D). Lower target cell–induced IFN-γ release (1700–1900 pg/ml) was obtained by these CAR-engineered NK cells when cocultured with $PC3^{PSCA}$. Of note, only PSCA-positive target cells stimulated $NK^{anti–PSCA-DAP12}$ cells to secrete high amounts of IFN-γ, whereas only basal cytokine release was observed in $NK^{myc-DAP12}$ control cells ($*p < 0.01$, $**p < 0.001$). Strikingly, even confrontation of $NK^{myc-DAP12}$ cells with HLA-B– or HLA-B/C–mismatched tumor cells did not cause enhanced IFN-γ release. In line with the results of the IFN-γ release assays, CAR-mediated lysis of target cells was again observed only after confrontation with PSCA-positive tumor cells (Fig. 7). In addition, nontransduced NK wt cells and $NK^{myc-DAP12}$ controls from the same donors did not react against $PC3^{PSCA}$, $H4^{PSCA}$ and also did not kill isogenic PC3 and H4 wt cells devoid of PSCA expression. Although $PC3^{PSCA}$ and $H4^{PSCA}$ cells expressed comparable levels of PSCA (Fig. 2A), the CAR-modified $NK^{anti–PSCA-DAP12}$ cells developed a stronger cytotoxic response against $H4^{PSCA}$, irrespective of whether the donors showed an HLA-C match and Bw4 mismatch (donors no. 1 and no. 3) or were HLA-B/C matched (donor no. 2). Intriguingly, when we probed CAR-engineered NK cells from donor no. 3 against RT4 and HT1376 cells, which both expressed lower levels of PSCA but had Bw6/C1 and Bw4/C2 mismatches, respectively, we revealed very strong cytotoxic reactions. Yet, no such cytotoxic reactions were monitored when using nontransduced NK cells and $NK^{myc-DAP12}$ cells. It therefore might be conceivable that in our experimental setting the HLA-C/KIR-mismatches to RT4 and HT1376 cells likely resulted in a decreased activation threshold of NK cells, which enabled an enhanced cytotoxic reaction of DAP12-CAR–modified NK cells when encountering $PSCA^{dim}$-target cells.

Discussion

Initial clinical trials with naturally occurring tumor-reactive T cells have proven that adoptive immunotherapy is a feasible and promising approach for cancer treatment (55). Limitations of this approach, such as HLA restriction or defective Ag presentation on tumor cells, and difficulties in raising sufficient numbers of tumor-reactive native T cells from patients, can be solved by the use of genetically modified autologous T cells with tumor-peptide TCRs or CARs (56, 57). So far, CARs have been designed for the redirection of T cells against various tumor Ags, such as CD30 on Hodgkin lymphoma cells (58), CEA on colorectal cancer cells (59), HER-2 on ovarian and breast cancer cells (60), TARP on prostate and breast cancer cells (61), and EGFRvIII and IL13R on glioblastoma cells (62–64). However, concern has been raised about genetically modified autoreactive T cells, which might cause undesirable side effects after infusion into patients. NK cells, in contrast, do not possess TCR-like molecules that might

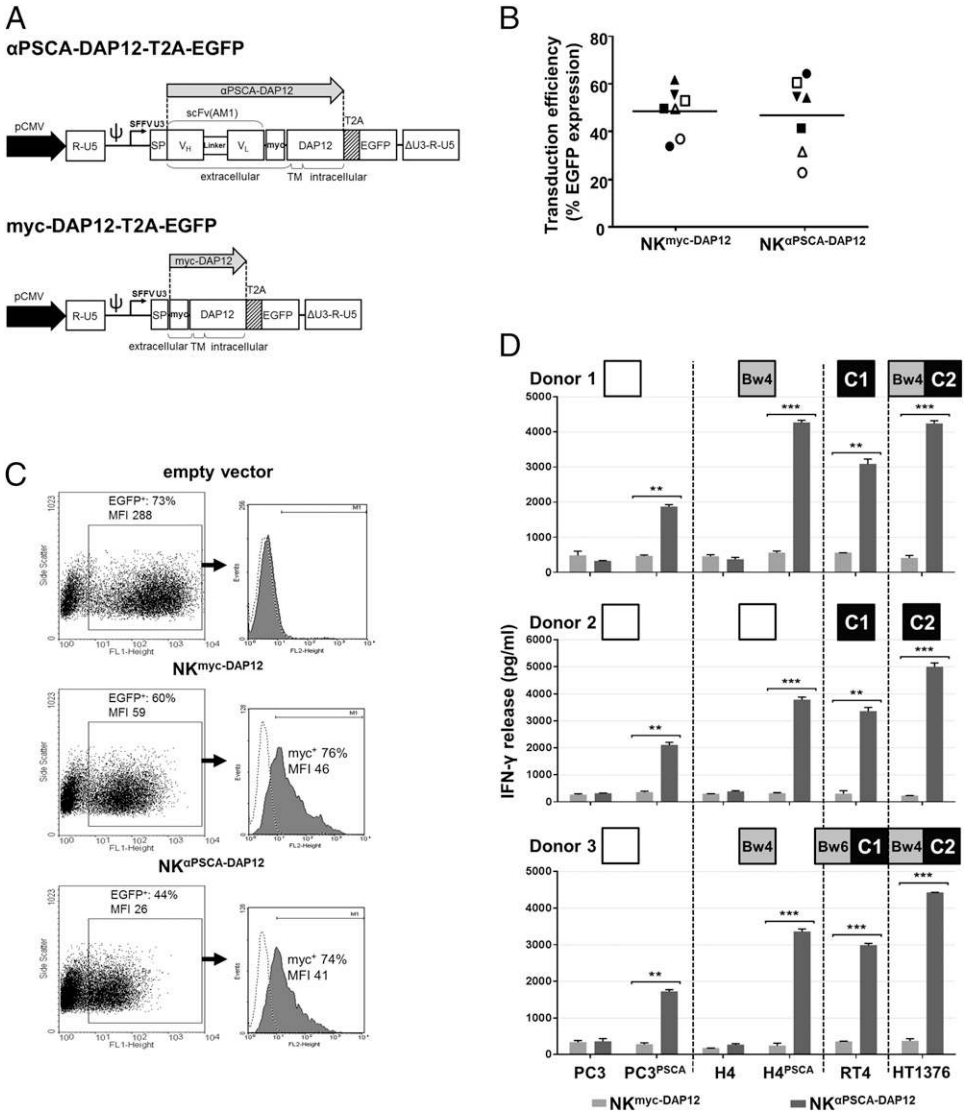

FIGURE 6. Human NK cells can be engineered with a DAP12-based CAR and release IFN-γ in the presence of PSCA-positive target cells. (**A**) Schematic representation of the coding sequences of anti–PSCA-DAP12 and myc-DAP12 (gray arrows) in the lentiviral pHATtrick vectors. The vectors contain a T2A cleavage site allowing simultaneous expression of the gene of interest and EGFP. (**B**) Transduction efficiencies of human primary NK cells. Depicted are the mean percentage of EGFP-positive cell fractions from seven different healthy donors. Geometric mean of transduction efficiencies using anti–PSCA-DAP12 and myc-DAP12 vectors is indicated. (**C**) Flow cytometry analysis of gene-modified NK cells. Cells were gated for EGFP expression and analyzed for anti–PSCA-DAP12 CAR and myc-DAP12 control surface expression. Cells were stained with anti–c-myc–biotin Ab and PE-labeled anti-biotin secondary Ab (gray histogram). Cells stained with IgG isotype Ab (open histogram) served as a control. As additional control, NK cells transduced with empty pHATtrick vector containing only EGFP were included. (**D**) Transduced NK cells were incubated with PSCA-positive tumor cell lines $PC3^{PSCA}$, $H4^{PSCA}$, corresponding isogenic PSCA-negative controls, and RT4 or HT1376 cells with endogenous expression of PSCA. HLA-mismatch predicting for a KIR-mismatch in the GvH direction is indicated (KIR-match in the GvH direction is represented by an open square). After 18 h of incubation, cell-free supernatant was harvested and the amount of released IFN-γ was measured by sandwich ELISA. Note the increase in IFN-γ release of anti–PSCA-DAP12 CAR–engineered NK ($NK^{anti–PSCA-DAP12}$) cells after cocultivation with PSCA-positive target cells (dark gray columns). Mean IFN-γ release of four single measurements and SEM are shown. $^{**}p < 0.01$, $^{***}p < 0.001$.

cause these unwanted immunological side effects. A number of studies have demonstrated that native NK cells are reactive against tumor cells in vitro and in vivo. Moreover, it has been shown that the NK cell lines NK92 and YT, as well as primary NK cells, can be engineered with CARs (21, 41–43, 65–68).

Whereas other approaches focused on the CD3ζ-chain as a signaling subunit in NK-redirecting CARs, our newly developed PSCA-specific CAR incorporated the signaling adaptor protein DAP12, which is involved in the signal transduction of activating NK cell receptors, in particular, NKG2C (26). Yet, some reports describing DAP12-deficient mice indicate that DAP12 associated with TREMs under special circumstances also transmits negative signals in cells of the myeloid lineage, such as macrophages and granulocytes (69). It has been proposed that a low-avidity interaction of TREMs with their so far unknown ligands might lead to incomplete DAP12 phosphorylation and somehow increases inhibitory signals (70). However, in our experimental settings using lymphoid NK cells, DAP12 was proven to efficiently induce cellular cytotoxicity when used as the signaling domain of a CAR, as discussed below.

To our knowledge, we report the first NK cell CAR containing DAP12 as an intracellular signaling domain. Additional costimulatory signaling fragments, which are frequently integrated into CARs (71), were not included owing to the anticipation that they are not necessary for DAP12-mediated NK cell activation. Of

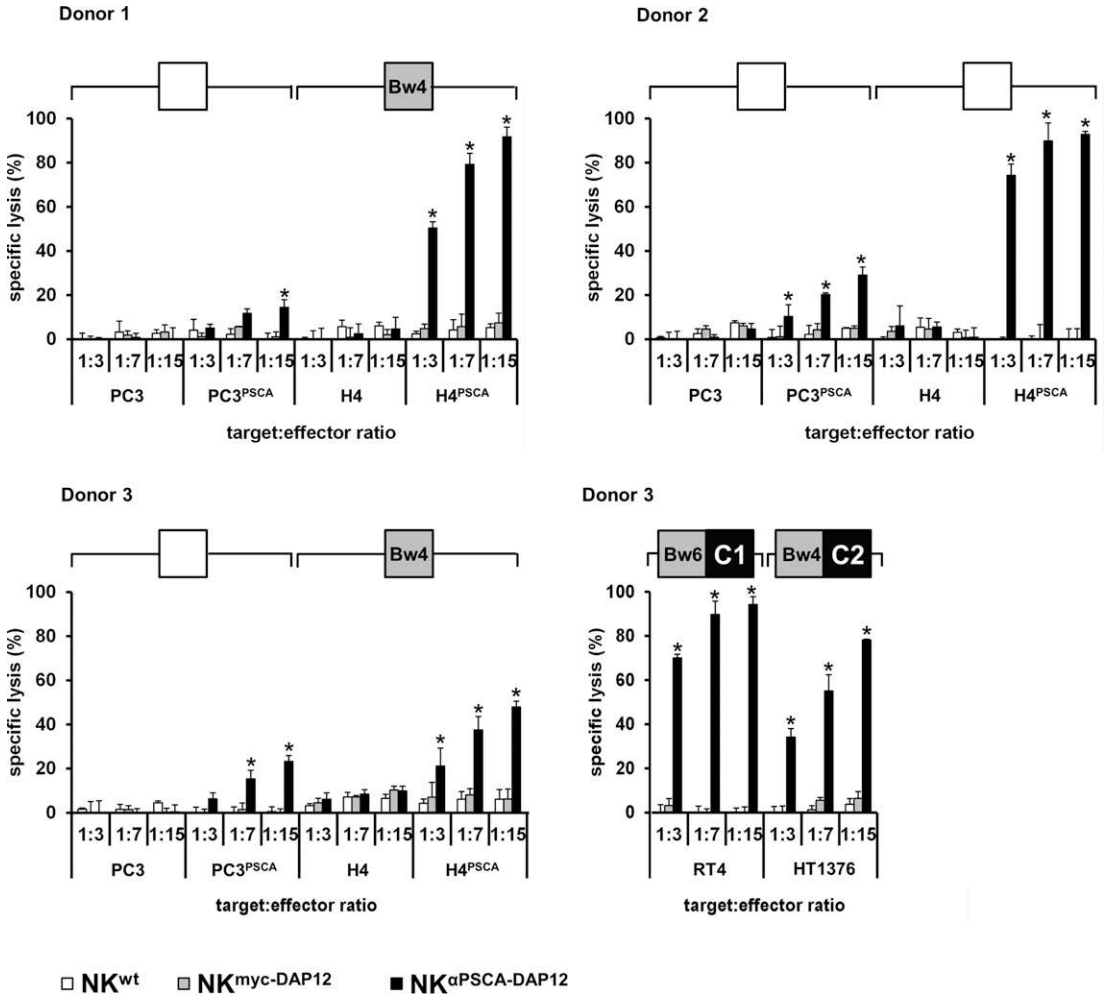

FIGURE 7. CAR-engineered primary human NK cells recognize and kill PSCA$^+$ tumor cells. Expanded primary NK cells from three different donors were transduced with anti–PSCA-DAP12 CAR or myc-DAP12 control. The gene-engineered NK$^{anti–PSCA-DAP12}$, NK$^{myc-DAP12}$, and nontransduced control cells were cocultured with PSCA-expressing tumor cells (PC3^{PSCA}, H4^{PSCA}) and isogenic PSCA-negative control cells (PC3, H4) at different target to effector ratios for 18 h. HLA-mismatch predicting for a KIR-mismatch in the GvH direction is indicated. The mean of specific tumor cell lysis and SD of triplets are shown. Gene-engineered NK cells from donor no. 3 were also incubated with the bladder carcinoma cell lines RT4 and HT1376, which show endogenous expression of PSCA. $*p < 0.05$.

interest, it appears that the DAP12-based CAR conferred a gradual improved cytotoxicity to YTS cells when compared with a CD3ζ-based CAR. So far it is tempting to speculate why a DAP12-based CAR containing only one ITAM might be at least as efficient in downstream signaling as a CD3ζ-based CAR containing three ITAMs. Yet, we suggest that ITAM phosphorylation of DAP12 might directly form a docking site for downstream signaling, whereas in the case of the CD3ζ-chain different phosphorylation grades might influence docking sites and eventually regulate the strength and different effector mechanisms of the NK cell response. That the ITAM domain of DAP12 was indispensable for the activation of NK cells was demonstrated using a phosphorylation-defective DAP12-ITAM, which fails to induce NK cell cytotoxicity after confrontation with PSCA-positive target cells.

Along with a strong and stable CAR expression of anti–PSCA-DAP12 in transduced YTS cells, we observed that the cross-linking of the CAR with PSCA caused an enhanced phosphorylation of the tyrosine protein kinase ZAP-70. As a likely consequence of ZAP-70–mediated signal induction, CAR-modified YTS cells released significantly increased amounts of IFN-γ when compared with controls. At the same time, no obvious correlation between the amounts of IFN-γ secretion by YTS cells and target Ag expression was detectable, which resembles results obtained by CD3ζ-CAR–modified NK92 cells engaging different ErbB2/HER-2-positive target cell lines (67). In line with the aforementioned observation, also the strength of the cytotoxic reaction as well as the IFN-γ release of CAR-modified primary NK cells was not directly correlated to the level of PSCA expression on target cells. Hence, we suggest that the observed dissimilar IFN-γ release after cocultivation of CAR-engineered YTS cells and primary NK cells with tumor cells not only is due to the level of PSCA expression but also might depend on the composition and expression levels of cell adhesion molecules and, in particular for primary NK cells, is linked to the lack of inhibitory HLA-B and -C molecules on target cells.

According to the results of the IFN-γ release assays, we revealed that YTS cells engineered with anti–PSCA-DAP12 CAR caused a highly specific lysis of only PSCA-positive target cells originating from prostate cancer, bladder carcinoma, and glioblastoma, whereas PSCA-negative tumor cells were not affected. Therefore, it can be concluded that the observed cytotoxic activity of PSCA-redirected YTS cells was exclusively due to the interaction of the PSCA-specific CAR with its Ag. In subsequent experimental NK immunotherapy, we demonstrated an antitumor effect of our DAP12-based CAR in a preclinical tumor model. To our knowl-

edge, we treated for the first time established solid tumors with CAR-modified NK cells, whereas other groups favored mixing of NK cells and target cells prior to tumor transplantation (23, 65–67) or chose an experimental setting that most likely confronts injected tumor cells and CAR-modified NK cells in the bloodstream or lung capillaries (67). In this article, we demonstrate that treatment with YTS$^{anti–PSCA-DAP12}$ NK cells resulted in a significantly delayed growth of PSCA-positive tumors when compared with tumors treated with YTS wt cells and YTS$^{myc-DAP12}$ controls, respectively. However, this significant antitumor effect was accomplished only by continuous injection of YTS$^{anti–PSCA-DAP12}$ cells. After termination of YTS$^{anti–PSCA-DAP12}$ treatment, 31% of mice remained tumor free, but in the remaining mice tumor growth accelerated, suggesting that injected YTS$^{anti–PSCA-DAP12}$ cells are short lived. This idea is further supported by our results showing lack of YTS$^{anti–PSCA-DAP12}$ engraftment in cured mice. Furthermore, our data suggest only a moderate tumor infiltration of YTS cells, which, in conjunction with other factors (i.e., differences in the vascularization of the tumors), might have resulted in the appearance of weak responders and nonresponders. In the future it might therefore be worthwhile to genetically modify NK cells with chemokine receptors to enhance selective tumor infiltration. That this kind of engrafted chemotaxis is beneficial was previously demonstrated by CXCR2- and CCR2-modified T cells, which showed improved tumor infiltrations and eradications in tumor xenograft models (72, 73).

In line with the results obtained with YTS NK cells, CAR-modified primary NK cells also showed a high and specific cytotoxicity toward PSCA-positive tumor cells, which, as mentioned above, was further enhanced by KIR ligand mismatches, particularly demonstrated using RT4 and HT1376 target cells having moderate PSCA expression levels. Although it is well known that in HLA-B and -C mismatches are important for the development of GvH disease in allogeneic hematopoietic stem cell transplantation (10, 11), we observed in our experiments that KIR/ligand mismatches in the GvH direction did not lead to increased cytotoxicity of nontransduced NK cells and genetically engineered NK$^{myc-DAP12}$ donor cells. Hence we assume that our 18-h protocol used for the cytotoxicity assays did not lead to the outgrowth of sufficient alloreactive NK cell numbers needed for induction of potent GvH reactions, which has been reported to require a longer period of time (17, 18).

In conclusion, when considering immunotherapy with DAP12-based CAR-modified NK cells, the use of autologous or allogeneic KIR/HLA-matched NK cells appears to be a promising and safe approach. In contrast, we suggest that the use of CAR-modified potentially alloreactive donor NK cells, which display a lower activation threshold, might be advantageous when targeting tumor cells with lower target Ag levels. If we consider the CAR-modified NK cells as short-lived effector cells, the latter approach appears feasible but still bears the risk of inherent GvH reactions.

In summary, we have shown that YTS-NK, as well as primary NK cells, can be successfully redirected against PSCA-positive tumors using a DAP12-based CAR. Furthermore, we showed that self-restriction of NK cells modified with a DAP12-based CAR can be surmounted when encountering PSCA-positive HLA-B/C– and HLA-C–matched tumor cells. We therefore conclude that DAP12-based CARs represent a promising tool for adjuvant immunotherapy.

Acknowledgments

We thank Dr. Galandrini, University “La Sapienza” (Rome, Italy), for providing the NK cell line YTS and F. Zachow, B. Goldberg, and K. Robel for excellent technical assistance.

Disclosures

The authors have no financial conflicts of interest.

References

1. Kalos, M., B. L. Levine, D. L. Porter, S. Katz, S. A. Grupp, A. Bagg, and C. H. June. 2011. T cells with chimeric antigen receptors have potent antitumor effects and can establish memory in patients with advanced leukemia. *Sci. Transl. Med.* 3: 95ra73.
2. Davila, M. L., R. Brentjens, X. Wang, I. Rivière, and M. Sadelain. 2012. How do CARs work?: Early insights from recent clinical studies targeting CD19. *OncoImmunology* 1: 1577–1583.
3. Brentjens, R. J., and K. J. Curran. 2012. Novel cellular therapies for leukemia: CAR-modified T cells targeted to the CD19 antigen. *Hematology (Am Soc Hematol Educ Program)* 2012: 143–151.
4. Brooks, A. G., J. C. Boyington, and P. D. Sun. 2000. Natural killer cell recognition of HLA class I molecules. *Rev. Immunogenet.* 2: 433–448.
5. Lanier, L. L. 2008. Up on the tightrope: natural killer cell activation and inhibition. *Nat. Immunol.* 9: 495–502.
6. Moretta, L., and A. Moretta. 2004. Unravelling natural killer cell function: triggering and inhibitory human NK receptors. *EMBO J.* 23: 255–259.
7. Colonna, M., F. Navarro, T. Bellón, M. Llano, P. García, J. Samaridis, L. Angman, M. Cella, and M. López-Botet. 1997. A common inhibitory receptor for major histocompatibility complex class I molecules on human lymphoid and myelomonocytic cells. *J. Exp. Med.* 186: 1809–1818.
8. Brooks, A. G., P. E. Posch, C. J. Scorzelli, F. Borrego, and J. E. Coligan. 1997. NKG2A complexed with CD94 defines a novel inhibitory natural killer cell receptor. *J. Exp. Med.* 185: 795–800.
9. Petrie, E. J., C. S. Clements, J. Lin, L. C. Sullivan, D. Johnson, T. Huyton, A. Heroux, H. L. Hoare, T. Beddoe, H. H. Reid, et al. 2008. CD94-NKG2A recognition of human leukocyte antigen (HLA)-E bound to an HLA class I leader sequence. *J. Exp. Med.* 205: 725–735.
10. Colonna, M., G. Borsellino, M. Falco, G. B. Ferrara, and J. L. Strominger. 1993. HLA-C is the inhibitory ligand that determines dominant resistance to lysis by NK1- and NK2-specific natural killer cells. *Proc. Natl. Acad. Sci. USA* 90: 12000–12004.
11. Ruggeri, L., M. Capanni, E. Urbani, K. Perruccio, W. D. Shlomchik, A. Tosti, S. Posati, D. Rogaia, F. Frassoni, F. Aversa, et al. 2002. Effectiveness of donor natural killer cell alloreactivity in mismatched hematopoietic transplants. *Science* 295: 2097–2100.
12. Hansasuta, P., T. Dong, H. Thananchai, M. Weekes, C. Willberg, H. Aldemir, S. Rowland-Jones, and V. M. Braud. 2004. Recognition of HLA-A3 and HLA-A11 by KIR3DL2 is peptide-specific. *Eur. J. Immunol.* 34: 1673–1679.
13. Uhrberg, M., N. M. Valiante, B. P. Shum, H. G. Shilling, K. Lienert-Weidenbach, B. Corliss, D. Tyan, L. L. Lanier, and P. Parham. 1997. Human diversity in killer cell inhibitory receptor genes. *Immunity* 7: 753–763.
14. Ruggeri, L., A. Mancusi, E. Burchielli, K. Perruccio, F. Aversa, M. F. Martelli, and A. Velardi. 2006. Natural killer cell recognition of missing self and haploidentical hematopoietic transplantation. *Semin. Cancer Biol.* 16: 404–411.
15. Gumperz, J. E., V. Litwin, J. H. Phillips, L. L. Lanier, and P. Parham. 1995. The Bw4 public epitope of HLA-B molecules confers reactivity with natural killer cell clones that express NKB1, a putative HLA receptor. *J. Exp. Med.* 181: 1133–1144.
16. Kärre, K. 1995. Express yourself or die: peptides, MHC molecules, and NK cells. *Science* 267: 978–979.
17. Colonna, M., E. G. Brooks, M. Falco, G. B. Ferrara, and J. L. Strominger. 1993. Generation of allospecific natural killer cells by stimulation across a polymorphism of HLA-C. *Science* 260: 1121–1124.
18. Rose, M. J., A. G. Brooks, L. A. Stewart, T. H. Nguyen, and A. P. Schwarer. 2009. Killer Ig-like receptor ligand mismatch directs NK cell expansion in vitro. *J. Immunol.* 183: 4502–4508.
19. Smyth, M. J., E. Cretney, J. M. Kelly, J. A. Westwood, S. E. Street, H. Yagita, K. Takeda, S. L. van Dommelen, M. A. Degli-Esposti, and Y. Hayakawa. 2005. Activation of NK cell cytotoxicity. *Mol. Immunol.* 42: 501–510.
20. Oshimi, Y., S. Oda, Y. Honda, S. Nagata, and S. Miyazaki. 1996. Involvement of Fas ligand and Fas-mediated pathway in the cytotoxicity of human natural killer cells. *J. Immunol.* 157: 2909–2915.
21. Müller, T., C. Uherek, G. Maki, K. U. Chow, A. Schimpf, H. G. Klingemann, T. Tonn, and W. S. Wels. 2008. Expression of a CD20-specific chimeric antigen receptor enhances cytotoxic activity of NK cells and overcomes NK-resistance of lymphoma and leukemia cells. *Cancer Immunol. Immunother.* 57: 411–423.
22. Chu, J., Y. Deng, D. M. Benson, S. He, T. Hughes, J. Zhang, Y. Peng, H. Mao, L. Yi, K. Ghoshal, et al. 2014. CS1-specific chimeric antigen receptor (CAR)-engineered natural killer cells enhance in vitro and in vivo antitumor activity against human multiple myeloma. *Leukemia* 28: 917–927.
23. Uherek, C., T. Tonn, B. Uherek, S. Becker, B. Schnierle, H. G. Klingemann, and W. Wels. 2002. Retargeting of natural killer-cell cytolytic activity to ErbB2-expressing cancer cells results in efficient and selective tumor cell destruction. *Blood* 100: 1265–1273.
24. Ford, J. W., and D. W. McVicar. 2009. TREM and TREM-like receptors in inflammation and disease. *Curr. Opin. Immunol.* 21: 38–46.
25. Bakker, A. B., E. Baker, G. R. Sutherland, J. H. Phillips, and L. L. Lanier. 1999. Myeloid DAP12-associating lectin (MDL)-1 is a cell surface receptor involved in the activation of myeloid cells. *Proc. Natl. Acad. Sci. USA* 96: 9792–9796.
26. Lanier, L. L., B. Corliss, J. Wu, and J. H. Phillips. 1998. Association of DAP12 with activating CD94/NKG2C NK cell receptors. *Immunity* 8: 693–701.

27. Campbell, K. S., S. Yusa, A. Kikuchi-Maki, and T. L. Catina. 2004. NKp44 triggers NK cell activation through DAP12 association that is not influenced by a putative cytoplasmic inhibitory sequence. *J. Immunol.* 172: 899–906.
28. Carr, W. H., D. B. Rosen, H. Arase, D. F. Nixon, J. Michaelsson, and L. L. Lanier. 2007. Cutting edge: KIR3DS1, a gene implicated in resistance to progression to AIDS, encodes a DAP12-associated receptor expressed on NK cells that triggers NK cell activation. *J. Immunol.* 178: 647–651.
29. Della Chiesa, M., E. Romeo, M. Falco, M. Balsamo, R. Augugliaro, L. Moretta, C. Bottino, A. Moretta, and M. Vitale. 2008. Evidence that the KIR2DS5 gene codes for a surface receptor triggering natural killer cell function. *Eur. J. Immunol.* 38: 2284–2289.
30. Hayley, M., S. Bourbigot, and V. Booth. 2011. Self-association of an activating natural killer cell receptor, KIR2DS1. *PLoS ONE* 6: e23052.
31. Lanier, L. L., B. C. Corliss, J. Wu, C. Leong, and J. H. Phillips. 1998. Immunoreceptor DAP12 bearing a tyrosine-based activation motif is involved in activating NK cells. *Nature* 391: 703–707.
32. Gumá, M., A. Angulo, C. Vilches, N. Gómez-Lozano, N. Malats, and M. López-Botet. 2004. Imprint of human cytomegalovirus infection on the NK cell receptor repertoire. *Blood* 104: 3664–3671.
33. Gumá, M., M. Budt, A. Sáez, T. Brckalo, H. Hengel, A. Angulo, and M. López-Botet. 2006. Expansion of CD94/NKG2C+ NK cells in response to human cytomegalovirus-infected fibroblasts. *Blood* 107: 3624–3631.
34. Kuijpers, T. W., P. A. Baars, C. Dantin, M. van den Burg, R. A. van Lier, and E. Roosnek. 2008. Human NK cells can control CMV infection in the absence of T cells. *Blood* 112: 914–915.
35. Morgenroth, A., M. Cartellieri, M. Schmitz, S. Günes, B. Weigle, M. Bachmann, H. Abken, E. P. Rieber, and A. Temme. 2007. Targeting of tumor cells expressing the prostate stem cell antigen (PSCA) using genetically engineered T-cells. *Prostate* 67: 1121–1131.
36. Dannull, J., P. A. Diener, L. Prikler, G. Fürstenberger, T. Cerny, U. Schmid, D. K. Ackermann, and M. Groettrup. 2000. Prostate stem cell antigen is a promising candidate for immunotherapy of advanced prostate cancer. *Cancer Res.* 60: 5522–5528.
37. Ross, S., S. D. Spencer, I. Holcomb, C. Tan, J. Hongo, B. Devaux, L. Rangell, G. A. Keller, P. Schow, R. M. Steeves, et al. 2002. Prostate stem cell antigen as therapy target: tissue expression and in vivo efficacy of an immunoconjugate. *Cancer Res.* 62: 2546–2553.
38. Saffran, D. C., A. B. Raitano, R. S. Hubert, O. N. Witte, R. E. Reiter, and A. Jakobovits. 2001. Anti-PSCA mAbs inhibit tumor growth and metastasis formation and prolong the survival of mice bearing human prostate cancer xenografts. *Proc. Natl. Acad. Sci. USA* 98: 2658–2663.
39. Reiter, R. E., Z. Gu, T. Watabe, G. Thomas, K. Szigeti, E. Davis, M. Wahl, S. Nisitani, J. Yamashiro, M. M. Le Beau, et al. 1998. Prostate stem cell antigen: a cell surface marker overexpressed in prostate cancer. *Proc. Natl. Acad. Sci. USA* 95: 1735–1740.
40. Lam, J. S., J. Yamashiro, I. P. Shintaku, R. L. Vessella, R. B. Jenkins, S. Horvath, J. W. Said, and R. E. Reiter. 2005. Prostate stem cell antigen is overexpressed in prostate cancer metastases. *Clin. Cancer Res.* 11: 2591–2596.
41. Elsamman, E. M., T. Fukumori, S. Tanimoto, R. Nakanishi, M. Takahashi, K. Toida, and H. O. Kanayama. 2006. The expression of prostate stem cell antigen in human clear cell renal cell carcinoma: a quantitative reverse transcriptase-polymerase chain reaction analysis. *BJU Int.* 98: 668–673.
42. Argani, P., C. Rosty, R. E. Reiter, R. E. Wilentz, S. R. Murugesan, S. D. Leach, B. Ryu, H. G. Skinner, M. Goggins, E. M. Jaffee, C. J. Yeo, J. L. Cameron, S. E. Kern, and R. H. Hruban. 2001. Discovery of new markers of cancer through serial analysis of gene expression: prostate stem cell antigen is overexpressed in pancreatic adenocarcinoma. *Cancer Res.* 61: 4320–4324.
43. Geiger, K. D., S. Hendruschk, E. P. Rieber, A. Morgenroth, B. Weigle, T. Juratli, V. Senner, G. Schackert, and A. Temme. 2011. The prostate stem cell antigen represents a novel glioma-associated antigen. *Oncol. Rep.* 26: 13–21.
44. Thomas-Kaskel, A. K., R. Zeiser, R. Jochim, C. Robbel, W. Schultze-Seemann, C. F. Waller, and H. Veelken. 2006. Vaccination of advanced prostate cancer patients with PSCA and PSA peptide-loaded dendritic cells induces DTH responses that correlate with superior overall survival. *Int. J. Cancer* 119: 2428–2434.
45. Waeckerle-Men, Y., E. Uetz-von Allmen, M. Fopp, R. von Moos, C. Böhme, H. P. Schmid, D. Ackermann, T. Cerny, B. Ludewig, M. Groettrup, and S. Gillessen. 2006. Dendritic cell-based multi-epitope immunotherapy of hormone-refractory prostate carcinoma. *Cancer Immunol. Immunother.* 55: 1524–1533.
46. Kiessling, A., M. Schmitz, S. Stevanovic, B. Weigle, K. Hölig, M. Füssel, S. Füssel, A. Meye, M. P. Wirth, and E. P. Rieber. 2002. Prostate stem cell antigen: identification of immunogenic peptides and assessment of reactive CD8 + T cells in prostate cancer patients. *Int. J. Cancer* 102: 390–397.
47. Cohen, G. B., R. T. Gandhi, D. M. Davis, O. Mandelboim, B. K. Chen, J. L. Strominger, and D. Baltimore. 1999. The selective downregulation of class I major histocompatibility complex proteins by HIV-1 protects HIV-infected cells from NK cells. *Immunity* 10: 661–671.
48. Amer, D. A., G. Kretzschmar, N. Müller, N. Stanke, D. Lindemann, and G. Vollmer. 2010. Activation of transgenic estrogen receptor-beta by selected phytoestrogens in a stably transduced rat serotonergic cell line. *J. Steroid Biochem. Mol. Biol.* 120: 208–217.
49. Zufferey, R., J. E. Donello, D. Trono, and T. J. Hope. 1999. Woodchuck hepatitis virus posttranscriptional regulatory element enhances expression of transgenes delivered by retroviral vectors. *J. Virol.* 73: 2886–2892.
50. Mochizuki, H., J. P. Schwartz, K. Tanaka, R. O. Brady, and J. Reiser. 1998. High-titer human immunodeficiency virus type 1-based vector systems for gene delivery into nondividing cells. *J. Virol.* 72: 8873–8883.
51. Kalajzic, I., M. L. Stover, P. Liu, Z. Kalajzic, D. W. Rowe, and A. C. Lichtler. 2001. Use of VSV-G pseudotyped retroviral vectors to target murine osteoprogenitor cells. *Virology* 284: 37–45.
52. Sutlu, T., S. Nyström, M. Gilljam, B. Stellan, S. E. Applequist, and E. Alici. 2012. Inhibition of intracellular antiviral defense mechanisms augments lentiviral transduction of human natural killer cells: implications for gene therapy. *Hum. Gene Ther.* 23: 1090–1100.
53. Burshtyn, D. N., J. Shin, C. Stebbins, and E. O. Long. 2000. Adhesion to target cells is disrupted by the killer cell inhibitory receptor. *Curr. Biol.* 10: 777–780.
54. Maghazachi, A. A. 2005. Insights into seven and single transmembrane-spanning domain receptors and their signaling pathways in human natural killer cells. *Pharmacol. Rev.* 57: 339–357.
55. Restifo, N. P., M. E. Dudley, and S. A. Rosenberg. 2012. Adoptive immunotherapy for cancer: harnessing the T cell response. *Nat. Rev. Immunol.* 12: 269–281.
56. Morgan, R. A., M. E. Dudley, J. R. Wunderlich, M. S. Hughes, J. C. Yang, R. M. Sherry, R. E. Royal, S. L. Topalian, U. S. Kammula, N. P. Restifo, et al. 2006. Cancer regression in patients after transfer of genetically engineered lymphocytes. *Science* 314: 126–129.
57. Rosenberg, S. A. 2008. Overcoming obstacles to the effective immunotherapy of human cancer. *Proc. Natl. Acad. Sci. USA* 105: 12643–12644.
58. Hombach, A., J. M. Muche, M. Gerken, S. Gellrich, C. Heuser, C. Pohl, W. Sterry, and H. Abken. 2001. T cells engrafted with a recombinant anti-CD30 receptor target autologous CD30(+) cutaneous lymphoma cells. *Gene Ther.* 8: 891–895.
59. Hombach, A., C. Schlimper, E. Sievers, S. Frank, H. H. Schild, T. Sauerbruch, I. G. Schmidt-Wolf, and H. Abken. 2006. A recombinant anti-carcinoembryonic antigen immunoreceptor with combined CD3zeta-CD28 signalling targets T cells from colorectal cancer patients against their tumour cells. *Gut* 55: 1156–1164.
60. Lindencrona, J. A., S. Preiss, T. Kammertoens, T. Schüler, M. Piechocki, W. Z. Wei, B. Seliger, T. Blankenstein, and R. Kiessling. 2004. CD4+ T cell-mediated HER-2/neu-specific tumor rejection in the absence of B cells. *Int. J. Cancer* 109: 259–264.
61. Hillerdal, V., B. Nilsson, B. Carlsson, F. Eriksson, and M. Essand. 2012. T cells engineered with a T cell receptor against the prostate antigen TARP specifically kill HLA-A2+ prostate and breast cancer cells. *Proc. Natl. Acad. Sci. USA* 109: 15877–15881.
62. Morgan, R. A., L. A. Johnson, J. L. Davis, Z. Zheng, K. D. Woolard, E. A. Reap, S. A. Feldman, N. Chinnasamy, C. T. Kuan, H. Song, et al. 2012. Recognition of glioma stem cells by genetically modified T cells targeting EGFRvIII and development of adoptive cell therapy for glioma. *Hum. Gene Ther.* 23: 1043–1053.
63. Kong, S., S. Sengupta, B. Tyler, A. J. Bais, Q. Ma, S. Doucette, J. Zhou, A. Sahin, B. S. Carter, H. Brem, et al. 2012. Suppression of human glioma xenografts with second-generation IL13R-specific chimeric antigen receptor-modified T cells. *Clin. Cancer Res.* 18: 5949–5960.
64. Sampson, J. H., B. D. Choi, L. Sanchez-Perez, C. M. Suryadevara, D. J. Snyder, C. T. Flores, S. K. Nair, R. J. Schmittling, E. A. Reap, P. K. Norberg, et al. 2014. EGFRvIII mCAR-modified T-cell therapy cures mice with established intracerebral glioma and generates host immunity against tumor-antigen loss. *Clin. Cancer Res.* 20: 972–984.
65. Esser, R., T. Müller, D. Stefes, S. Kloess, D. Seidel, S. D. Gillies, C. Aperlo-Iffland, J. S. Huston, C. Uherek, K. Schönfeld, et al. 2012. NK cells engineered to express a GD2-specific antigen receptor display built-in ADCC-like activity against tumour cells of neuroectodermal origin. *J. Cell. Mol. Med.* 16: 569–581.
66. Kruschinski, A., A. Moosmann, I. Poschke, H. Norell, M. Chmielewski, B. Seliger, R. Kiessling, T. Blankenstein, H. Abken, and J. Charo. 2008. Engineering antigen-specific primary human NK cells against HER-2 positive carcinomas. *Proc. Natl. Acad. Sci. USA* 105: 17481–17486.
67. Schonfeld, K., C. Sahm, C. Zhang, S. Naundorf, C. Brendel, M. Odendahl, P. Nowakowska, H. Bonig, U. Kohl, S. Kloess, et al. 2015. Selective inhibition of tumor growth by clonal NK cells expressing an ErbB2/HER2-specific chimeric antigen receptor. *Mol. Ther.* 23: 330–338.
68. Schirrmann, T., and G. Pecher. 2002. Human natural killer cell line modified with a chimeric immunoglobulin T-cell receptor gene leads to tumor growth inhibition in vivo. *Cancer Gene Ther.* 9: 390–398.
69. Hamerman, J. A., N. K. Tchao, C. A. Lowell, and L. L. Lanier. 2005. Enhanced Toll-like receptor responses in the absence of signaling adaptor DAP12. *Nat. Immunol.* 6: 579–586.
70. Turnbull, I. R., and M. Colonna. 2007. Activating and inhibitory functions of DAP12. *Nat. Rev. Immunol.* 7: 155–161.
71. Sadelain, M., R. Brentjens, and I. Rivière. 2009. The promise and potential pitfalls of chimeric antigen receptors. *Curr. Opin. Immunol.* 21: 215–223.
72. Craddock, J. A., A. Lu, A. Bear, M. Pule, M. K. Brenner, C. M. Rooney, and A. E. Foster. 2010. Enhanced tumor trafficking of GD2 chimeric antigen receptor T cells by expression of the chemokine receptor CCR2b. *J. Immunother.* 33: 780–788.
73. Moon, E. K., C. Carpenito, J. Sun, L. C. Wang, V. Kapoor, J. Predina, D. J. Powell, Jr., J. L. Riley, C. H. June, and S. M. Albelda. 2011. Expression of a functional CCR2 receptor enhances tumor localization and tumor eradication by retargeted human T cells expressing a mesothelin-specific chimeric antibody receptor. *Clin. Cancer Res.* 17: 4719–4730.